Bull Mar Sci. 94(1):47–71. 2018
https://doi.org/10.5343/bms.2017.1060

research paper

Genetic population structure of the spotted seatrout (*Cynoscion nebulosus*): simultaneous examination of the mtDNA control region and microsatellite marker results

Seifu Seyoum [1]*
Richard S McBride [2]
Michael D Tringali [1]
Vicki L Villanova [3]
Cecilia Puchutulegui [1]
Samantha Gray [1]
Nathan Van Bibber [1]

[1] *Florida Fish and Wildlife Conservation Commission, Fish and Wildlife Research Institute, 100 Eighth Avenue Southeast, St. Petersburg, Florida 33701.*

[2] *National Marine Fisheries Service, Northeast Fisheries Science. Center, 166 Water Street, Woods Hole, Massachusetts 02543.*

[3] *Harris County Institute of Forensic Sciences, Forensic Genetics Laboratory, 2450 Holcombe Boulevard, Suite 7 Houston, Texas 77021.*

* *Corresponding author email: <seifu.seyoum@myfwc.com>.*

Date Submitted: 15 May, 2017.
Date Accepted: 17 October, 2017.
Available Online: 21 November, 2017.

ABSTRACT.—The spotted seatrout, *Cynoscion nebulosus* (Cuvier, 1830), lives almost entirely within natal estuaries, and although many genetic studies identify fine-scale population structure, they do not provide a consensus as to the number of stocks, the stock boundaries, or their connectivity. Two perceived limitations of previous studies were addressed. To address a presumption of limited sampling, we assembled a large sample size with broad geographic range: 547 specimens from 18 sampling areas (mean inter-area distance = 270 km) between Texas and North Carolina, representing the majority of this species' range. To address the presumptive limitations of genetic markers, two genetic marker types were compared: a 335-base-pair segment of the mitochondrial DNA (mtDNA) control region and 38 microsatellite loci. MtDNA haplotype frequencies were different only between populations of the Gulf of Mexico (GoM) and the Atlantic Ocean, but not between the western GoM and the eastern GoM. In contrast, the microsatellite loci characterized the species' range-wide population structure as three geographically non-overlapping clusters. These clusters were defined by two genetic breaks: one at the Apalachicola River, on Florida's Gulf Coast, and another in the Atlantic Ocean between Miami and Palm Beach on Florida's east coast. Moreover, within each genetic cluster (identified by microsatellite markers), a pattern of isolation by distance was evident. This new characterization of spotted seatrout population structure supports assessment and management of the species by individual states and defines distinct stock boundaries in Florida, the only state with multiple genetic stocks, as defined by either genetic marker type.

Spotted seatrout, *Cynoscion nebulosus* (Cuvier, 1830), is a widely distributed coastal finfish, ranging from the temperate zone of the Atlantic Ocean (Massachusetts, USA), through the subtropical zone of the southeastern United States, to the tropical zones of the Florida Keys and the Gulf of Mexico (GoM; Campeche Bay, Mexico). It supports economically important fisheries from the Chesapeake Bay to Texas (Pearson 1929), which today are primarily recreational (NMFS 2014).

Spotted seatrout adults spawn almost entirely in coastal embayments (Pearson 1929), larvae have a short planktonic existence (<14 d; Peebles and Tolley 1988), and individuals rarely travel >48 km from their natal estuary (Moffett 1961, Iversen and Moffett 1962). Short-distance dispersal restricts gene flow between adjacent estuaries and leads to fine-scale population structure. Growth information has been examined in relation to population structure but with conflicting results, and no other phenotypic traits (e.g., morphometrics) have been tied to its population structure (McBride 2014). Genetic evidence of isolation by distance has led to acceptance of fine-scale (e.g., at the state level) assessment and management of spotted seatrout in the United States (McBride 2014).

Isolation by distance may be accompanied with distinct genetic breaks at a coarser, regional scale in coastal ecosystems due to hydrodynamic discontinuities that influence the phylogeography of individual fish species (Eble et al. 2015). In the scheme of Briggs and Bowen (2012), the geographic distribution of spotted seatrout overlaps at least three biogeographic zones that could represent such discontinuities. A northern zone of the western North Atlantic Ocean extends from the Canadian Maritime to Cape Hatteras, North Carolina, encompassing the marine fauna at boreal and temperate latitudes. In the subtropics, a Carolina Province is split into two parts on either side of Florida: one extending from Cape Hatteras to Cape Canaveral, in east-central Florida on the Atlantic side; and from Cape Romano, in southwest Florida, to Cape Rojo, Mexico, on the GoM side. In the tropics, the Caribbean Province extends from Capes Canaveral and Romano to the Amazon and includes Bermuda.

Such a broad distribution of spotted seatrout, across many biogeographical divisions, may be accompanied by population boundaries in association with some of these biogeographic boundaries. For example, a genetic break has been observed in association with the southern tip of Florida for estuarine fishes [e.g., bonnethead shark, *Sphyrna tiburo* (Linnaeus, 1758)—Escatel-Luna et al. 2015; sheepshead, *Archosargus probatocephalus* (Walbaum, 1792)—Seyoum et al. 2017); and reef fishes: black sea bass, *Centropristis striata* (Linnaeus, 1758)—McCartney et al. 2013; hogfish, *Lachnolaimus maximus* (Walbaum, 1792)—Seyoum et al. 2015]. A vicariant zone has been proposed as an additional population boundary in the northern GoM (McClure and McEachran 1992). Finally, one might expect differences in genetic distance between as well as within these populations, as have been observed in small estuarine fishes with limited dispersal capabilities, such as Gulf killifish, *Fundulus grandis* Baird and Girard, 1853 (Williams et al. 2008), and Atlantic silverside, *Menidia* spp. (Mach et al. 2011).

There is considerable information on the genetic structure of spotted seatrout. In fact, a series of investigations into its genetic population structure capture major milestones in terms of advancing methods of population genetics (Online Table S1). Initially, variations in general proteins (Weinstein and Yerger 1976) and allozymes (King and Pate 1992, King and Zimmerman 1993) revealed a pattern of isolation by distance in both the GoM and Atlantic Ocean, although that was not reciprocated

by the work of Ramsey and Wakeman (1987). Gold and Richardson (1998), using restriction fragment length polymorphism (RFLP) of the mtDNA, identified distinct genetic populations in Texas and in the GoM and Atlantic basins, including significant subdivisions in the GoM region, though this was not affirmed by a later study (Gold et al. 1999).

The mtDNA control region sequencing has more polymorphisms and potentially could reveal better delineation of the stock structure. However, only one study of the spotted seatrout employed this method and detected isolation by distance, but not discrete populations (Anderson and Karel 2009). In a follow-up study, Anderson and Karel (2010) included microsatellite markers and asserted the existence of at least three subpopulations in Texas waters. But no study of the control region variation in spotted seatrout had included specimens from both GoM and Atlantic regions.

Use of microsatellite markers to date has led to conflicting results: Gold et al. (2003) reported no differentiation of populations in a limited range (approximately 560 km) of Texas, whereas Anderson and Karel (2009, 2010) found isolation by distance within the same area using both microsatellite markers and control region sequencing. Similarly, Somerset and Saillant (2014) found an isolation-by-distance pattern in the northern GoM region along a 466-km stretch of the coast, whereas O'Donnell et al. (2014) found a weakly defined genetic break at New River, North Carolina, between Georgia and North Carolina (approximately 750 km). On the other hand Wiley and Chapman (2003) and Ward et al. (2007) found significant genetic breaks among samples separated by known zoogeographic barriers; however, the differences were contrary to phylogeographic expectations because samples on either side of the geographic boundaries showed less differentiation than samples within geographic boundaries (see Online Table S1).

In summary, a wide range of molecular tools have been used to investigate this species. Individually, some have identified a range-wide pattern of isolation by distance, or localized subpopulation structure. However, collectively, these results have been conflicting, and the number and boundaries of spotted seatrout populations is still debatable among fisheries managers. The earliest studies demonstrated, in a pioneering manner, that this species exhibits isolation by distance in coastal marine systems, but they did not report consistent genetic breaks across the seascape. Other studies, focused within one biogeographic zone, or even one state, were often designed to examine suitable sources for aquaculture or stock enhancement, and were not designed to advance a comprehensive definition of stock structure. For all these reasons, a more complete meta-analysis of this rich history was not likely to help characterize the number and boundaries of genetic populations of spotted seatrout.

For a comprehensive characterization of the spotted seatrout genetic population structure, we sampled more fish, at more locations, and at more microsatellites loci, than any previous study. We used two complementary analytical methods: (1) the mtDNA control region to examine for deep divergence, and (2) a large number of microsatellite DNA loci to reveal finer-scale patterns of genetic structure for a comprehensive analysis of this coastal marine fish.

Materials and Methods

Sampling and DNA Extraction.—Specimens were collected from 18 sampling areas from Texas to North Carolina (Fig. 1). A large collection on three separate

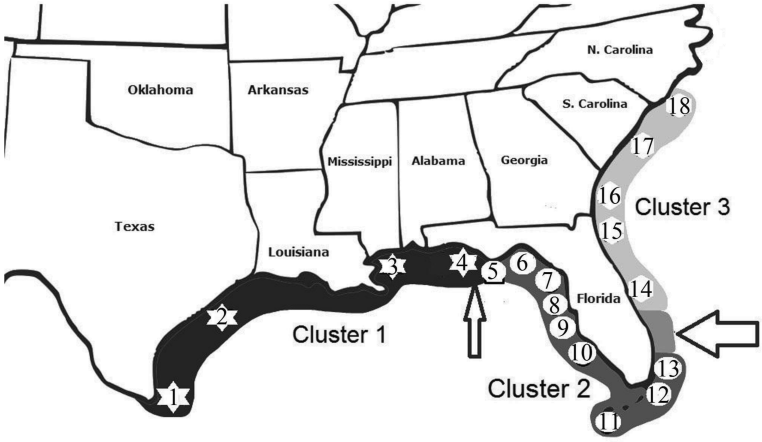

Figure 1. Sampling areas of spotted seatrout (*Cynoscion nebulosus*) for the study of genetic population structure for both mtDNA control region and 38 microsatellite DNA loci: 1 = South Padre Island, 2 = Port Arthur, 3 = Pascagoula, 4 = Fort Walton, 5 = Apalachicola, 6 = Steinhatchee, 7 = Cedar Key, 8 = Tarpon Springs, 9 = Tampa Bay, 10 = Charlotte Harbor, 11 = Big Pine Keys, 12 = Florida Bay, 13 = Biscayne Bay, 14 = Sebastian Inlet, 15 = St. Johns River, 16 = St. Andrew, 17 = Charleston, 18 = Morehead City. Specimens were collected sporadically from 1995 through 2000 and an additional collection was made from Cedar Key in 2002 and in 2010. The boundaries of the three spotted seatrout clusters inferred from STRUCTURE analysis are marked by different shades. Arrows indicate regions of gene flow restriction (i.e., a genetic break) between western and eastern Gulf of Mexico (clusters 1 and 2) and eastern Gulf of Mexico and Atlantic Ocean (clusters 2 and 3).

dates were made from Cedar Key for the microsatellite markers initial analyses. The average distance between sampling areas was 266 km (range: 69–788 km). Fish were collected from 1996 through 2000 (Online Table S2) within the same generation interval (4–5 yrs) except one from Cedar Key in 2010. A small piece of muscle tissue was excised from each fish, wrapped in aluminum foil, and frozen until processed, or a piece from the fin was excised, placed in 70% ethanol, and stored at room temperature until processed. Genomic DNA was extracted using the PureGene DNA isolation kit following manufacturer's instructions (Gentra Systems Inc., Minneapolis, MN) and was rehydrated in 50 µl of deionized water. In total, 547 fish were sampled, a mean of 25.5 per sampling area (excluding Cedar Key, to avoid bias) (range: 20–29).

mtDNA Control Region Sequencing.—Polymerase chain reaction (PCR) of the control region was performed using general primers L-15926 (Kocher et al. 1989) and H16498 (Meyer et al. 1990) and Promega Taq (Promega Corporation, Madison, WI) in a DeltaCycler II System (Ericomp Inc., San Diego, CA), as described by Kocher et al. (1989). The resulting amplicons were cloned and sequenced as described in Seyoum et al. (2000). From these sequences, internal primers designated L– (5′–CTAGCATTCTAAACTAAACTACTCTTTGATG–3′) and H– (5′–GCCAGGAATAATTCACTGTGTGAAACCCCC–3′) were designed. PCR of the mtDNA control region of the 547 individuals was performed using the above internal primers (Kocher et al. 1989). The amplicons were gel-purified (Agilent Technologies, Santa Clara, CA) and sequenced from both directions using Big Dye Terminator v1.1 (Applied Biosystems, Inc.). The cycle-sequenced products were precipitated and resuspended in Hi-Di Formamide and visualized on a 3130 Genetic Analyzer (Applied

Biosystems, Inc.). Sequences were aligned and edited using Sequencer (v4.9; Gene Codes Corporation, Ann Arbor, Michigan).

Control Region Data Analysis.—The control region sequence of 547 specimens was analyzed in MEGA7 (v7.0, Tamura et al. 2013) to generate a pairwise matrix of sequence divergence values between pairs of individuals, to construct an unrooted neighbor-joining tree, and to determine the confidence probability of the branch lengths on the tree. The TN93 Tamura-Nei model was selected for subsequent analyses based on the Akaike information criterion (AICc) lowest score using the model test program implemented in MEGA. The various molecular indices for the control region were determined using DnaSP (v5, Librado and Rozas 2009).

Individual- and within-population variance could not be partitioned and properly represented by eigenvectors when genetic variation is summarized by sampling areas. To reveal the internal structure, that is, within-population variance, we calculated the pairwise individual genetic distance of the 547 sequences using MEGA7 under the option of Tamura-Nei distance and used these matrices to conduct a principal-component analysis (PCA) plot (GenAlEx v6.5; Peakall and Smouse 2006, 2012). To assess variation among populations, we calculated pairwise sampling area Φ_{ST} values as implemented in Arlequin (v3.5.; 1000 permutations; Excoffier and Lischer 2010) and conducted PCA (GenAlEx) to plot the relationships among the sampling areas. The magnitude of genetic structure among and between groupings of sampling areas was determined via analysis of molecular variance (AMOVA) using the program Arlequin. The proportions of variation were computed following an a priori hierarchical approach at various levels, among regions (Φ_{CT}), within regions (Φ_{SC}), and within sampling areas (Φ_{ST}), and the Φ statistic was assessed by the permutation method as implemented in Arlequin. The variance components used to calculate Φ-statistics are analogous to Wright's *F*-statistics (Excoffier et al. 1992) and are calculated in the same way in AMOVA. Wright's *F*-statistics is related as $\theta = F_{ST}$ and we retained the θ notation to avoid confusion about *F*-statistics (Weir and Cockerham 1984). The a priori hierarchical approach of the AMOVA was based on the PCA grouping of the sampling areas of the western GoM, eastern GoM, and Atlantic regions as it is a multivariable method for exploring data to reveal variations among individuals within populations and by extension among populations prior to any assumptions.

The population demographic history of the spotted seatrout was examined based on the observed and expected mismatch distribution of the control-region-sequence pairwise differences on the assumptions of constant population size (Slatkin and Hudson 1991) and growing and declining populations (Rogers and Harpending 1992) as implemented in DnaSP. The basic demographic parameters theta initial θ_0 and theta final θ_1 (before and after demographic changes) and τ (tau, the date of growth or decline measured in units of mutational time and the raggedness index; Harpending 1994) were calculated in Arlequin (parametric bootstrap with 10,000 replicates). In addition, Tajima's *D* test, Fu and Li's *D*-test statistic, Fu and Li's *F* statistics were calculated as implemented in DnaSP. Negative values in these measures signify demographic expansion. The pairwise mismatch distributions data for the Atlantic, GoM, and combined samples and lineage 1 were graphed using SigmaPlot 2012 (Systat Corporation, Inc.).

Microsatellite DNA Loci Genotyping.—All specimens sequenced for the control region of the mtDNA were genotyped for 38 microsatellite DNA loci, 27 of which were developed in our laboratory specifically for this species (Cneb- used by Seyoum et al. 2013) and 11 from red drum [(Soc099, –133, and –243; Turner et al. 1998): (Soc415, –416, –426, –532, –564, –568, –635, and –660; Renshaw et al. 2009)] (see Appendix 1). Multiplex PCR amplifications for each specimen were carried out in an Eppendorf thermal cycler containing 50–100 ng of total DNA, 10 µl of 1.25 mM dNTP mix, 0.25 µl of 0.1 mg ml^{-1} BSA, a combination of three optimally selected primers of three loci with each forward primer labeled with a unique fluorescent dye, 5 µl of *Taq* polymerase buffer (10×) containing 2.5 mM $MgCl_2$ (Promega), and 1.25 units of *Taq* polymerase (Promega). Optimal primers were chosen based on minimum primer dimerization, different sizes and the similar annealing temperature. The reaction profile was 94 °C for 2 min, 35× (94 °C for 35 s, 55 °C for 35 s, 72 °C for 35 s), and final extension at 72 °C for 30 min. Fragments were visualized on an ABI 3130 XL genetic analyzer and genotyped using GeneMapper (v4.0, Applied Biosystems, Inc.). A Gene Scan-500 ROX-labeled size standard was used for fragment assays.

Microsatellite DNA Statistical Analyses.—We used Micro-Checker software (Van Oosterhout et al. 2004) to assess the quality of our microsatellite scoring for null alleles, stutters, and allele dropouts. Genotypic disequilibrium was examined for each sampling area using Genepop (Rousset 2008). Hardy-Weinberg equilibrium (HWE) expectations and observed (H_O) and unbiased expected (H_E) heterozygosity estimates were calculated using Genepop. The critical *P* value was performed using Benjamini and Hochberg (1995) correction. The polymorphic information content (PIC) was estimated as implemented in the program Cervus (v3.0., Kalinowski et al. 2007). Genetic diversity, number of alleles, and allelic richness were calculated over all loci in each sampling area using the program FSTAT (v2.9., Goudet 2001). To explore variation among individual within-populations to reveal internal structure using microsatellite markers, factorial correspondence analysis (FCA) (GENETIX v4.02, Belkhir et al. 2000) was conducted. From this analysis, the individual genotypes were plotted into two-dimensional space based on the genetic relationships observed at the 38 microsatellite loci. The D_A distance (Nei et al. 1983) produces the greatest probability of obtaining the correct branching pattern among closely related populations (Takezaki and Nei 1996, 2008). For this reason, the pairwise sampling area D_A was calculated using the software POPTREE2 (Takezaki et al. 2010). The estimates were then used to make a plot of the sampling areas in the PCA as explained above for the mtDNA sequence data. The magnitude of genetic structure among groupings of sampling areas was determined via AMOVA using Arlequin also as described above.

Distances in kilometers between sampling areas were estimated by measuring the shortest points following the coastline in Google Earth. To test whether the genetic relationships of specimens among sampling areas fit the pattern of isolation by distance, we estimated the Mantel correlation between genetic distance (Φ_{ST} for the mtDNA control region and D_A for microsatellite markers) and geographic distance (km) using the program GenAlEx (9999 randomization).

To examine the naturally occurring genetic clusters of individuals of the sampling areas, we used the Bayesian clustering algorithm employed by STRUCTURE (v2.3.4, Pritchard et al. 2000). In this model, individuals were probabilistically assigned

to one or more clusters (K) in the manner that minimized deviation from Hardy-Weinberg equilibrium and linkage disequilibrium between genotypes. Ten replicate simulations were conducted using 3.0×10^6 Markov-Chain Monte Carlo (MCMC) simulations after a 1.0×10^6 burn-in period for each value of K from 1 (the null hypothesis of panmixia) to 18 (complete fragmentation into distinct genetic clusters). We used the admixture model and independent-allele-frequencies option to minimize overestimating the number of groups present in the data set (Pritchard et al. 2009). The output file for 10 replicate runs from STRUCTURE was uploaded into the Web-based software STRUCTURE HARVESTER (Earl and vonHoldt 2012). STRUCTURE HARVESTER utilizes the posterior probabilities from STRUCTURE to calculate *lnP(D)* and the magnitude change of *lnP(D)*, that is, the log likelihood for each K, relative to the standard deviation, called ΔK (Evanno et al. 2005). After the most likely number of clusters had been identified, the average proportional cluster and individual membership from the 10 replicate runs were aligned and summarized using the program CLUMPP (v1.1.2, Jakobsson and Rosenberg 2007) under the Greedy algorithm with 1000 replicates.

Results

Control Region Genetic Variation.—A 335-base-pair (335-bp) fragment of the mtDNA control region was sequenced for 547 specimens of spotted seatrout collected from 18 sampling areas. All sequence mutations recorded in the spotted seatrout were in the form of single-bp substitutions except in two individuals that showed single-bp indels. The molecular indices for the control region are summarized in Online Table S2. There were 119 polymorphic sites (mean = 27), 266 haplotypes (mean = 22) over all sampling area, and 5.4 nucleotide site differences between individuals. The average nucleotide diversity and haplotype diversity were 0.014 and 0.96, respectively.

Genetic Structure Based on Control Region.—Construction of the neighbor-joining tree of specimens of each sampling area and the combined showed the presence of two major non-overlapping lineages separated by a high interior branch test (Online Table S2, Fig. 2). This tree does not show a clear geographical split between GoM and Atlantic sampling areas. However, the overall haplotype lineage distribution was phylogeographically structured, being significantly different between the GoM and the Atlantic sampling areas ($\chi^2 = 70.4$, df = 1, $P < 0.00001$). The distribution also showed highly significant difference among the western GoM, eastern GoM, and Atlantic specimens ($\chi^2 = 25.81$, df = 2, $P < 0.00001$). There was, however, no significant difference in lineage distribution between the between western and eastern GoM specimens ($\chi^2 = 0.0002$, $P = 0.989$).

Analysis of the PCA plot to assess variation among the 547 individuals showed only the western GoM specimens, not the eastern GoM, were separated with little overlap from the Atlantic specimens by PC2, which explained only 12.3% of the total variation, whereas the eastern and western GoM samples were not separated by PC1 or PC2 (Fig. 3A). In the PCA plot based on the pairwise 18 sampling areas Φ_{ST} values (Table 1, above diagonal), PC1 explained 93.2% of the genetic variation and PC2 explained 4.8% (Fig. 3B). The scattergram strongly, but not completely, separated the

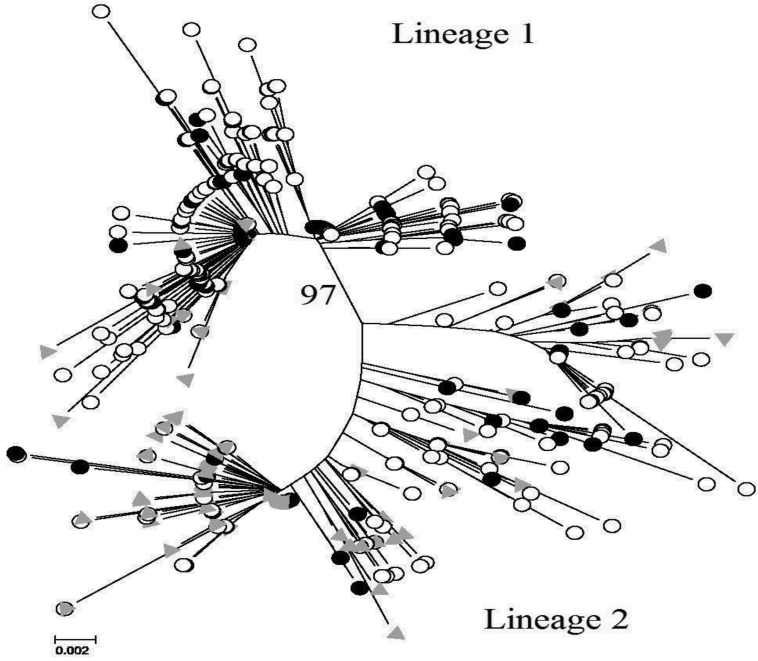

Figure 2. Unrooted neighbor-joining tree of mtDNA control region sequence haplotypes of the 547 individuals implemented in MEGA. Two lineages divided by a 97% bootstrap value are depicted in a radial view. Black circles represent western Gulf of Mexico specimens, white circles represent eastern Gulf of Mexico specimens, and gray triangles represent Atlantic specimens.

GoM and Atlantic sampling areas, whereas the western and eastern GoM sampling areas were not separated by either PC1 or PC2.

The overall control region sequence AMOVA result indicated the presence of significant differentiation among the sampling areas (Φ_{ST} = 0.098, P < 0.0001) due to highly significant among-group variance when the sampling areas were grouped into GoM (1–13) and Atlantic (14–18) (Φ_{CT} = 0.186, P < 0.0001; Table 2). No genetic differentiation was indicated within or between the western and eastern GoM sampling areas. The results of AMOVA is highly complementary to the analysis of the distribution of the lineages and the PCA, and overall the control region strongly, but not completely, indicated a deep divergence between the GoM and Atlantic sampling areas. This is because the adjoining sampling areas between the GoM and Atlantic areas (13 and 14) are not spatially separated as indicated by the PCA. Furthermore, in a two-group AMOVA, a highly significant genetic distance was found, not only between the GoM and Atlantic sampling areas (Φ_{CT} = 0.186, P < 0.00001), but also when sampling area 14 was included in the GoM group against the remaining Atlantic sampling areas 15–18 (Φ_{CT} = 0.211, P < 0.00001). The control region analysis, therefore, did not completely separate the GoM and Atlantic sampling areas, probably due to limited sample size involving sampling areas 13 and 14.

There was no correlation between the pairwise geographic and genetic distances (Φ_{ST}, mtDNA) of sampling areas within the GoM (P = 0.110, R = 0.208), or within the Atlantic (P = 0.230, R = 0.482). However, there was a significant correlation over the entire region of the 18 sampling areas (P = 0.001, R = 0.513), but this is attributed to

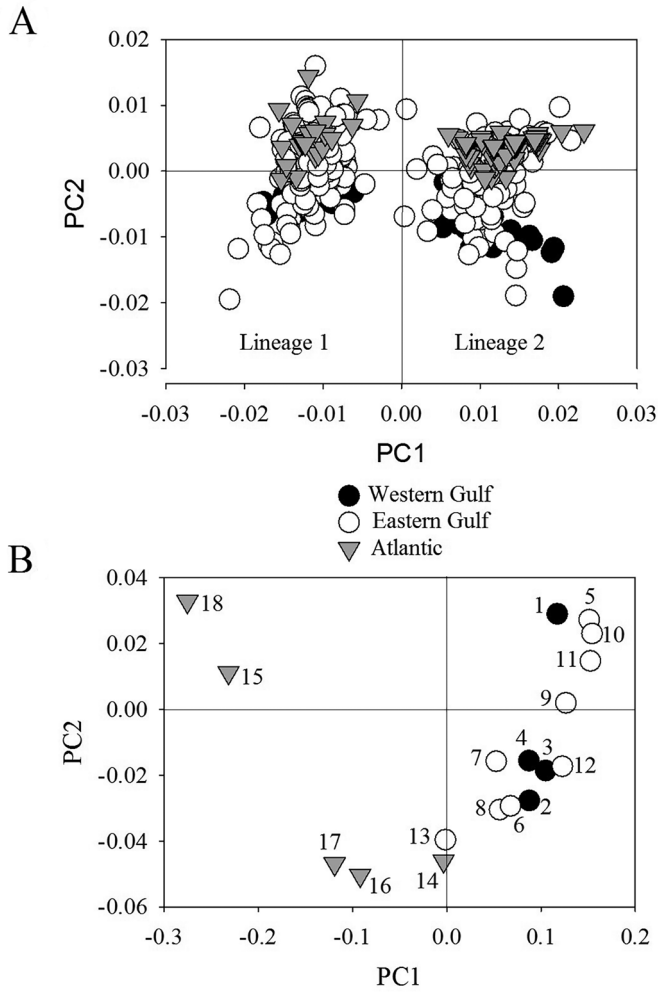

Figure 3. Principal coordinate analysis of the mtDNA (for spotted seatrout, *Cynoscion nebulosus*) control sequence data based on (A) haplotypic similarity matrix overall samples of the 547 individual pairwise Tamura-Nei distance, (B) nonstandardized distance method of a matrix of 18 pairwise sampling area Φ_{ST} from Texas to North Carolina. Sampling areas numbered as in Figure 1.

the genetic break between the GoM and Atlantic samples rather than isolation by distance.

The demographic analysis for the Atlantic, GoM, and both geographic regions' control region pairwise nucleotide differences showed a bimodal curve and a low Harpending's raggedness index, ranging from 0.01 to 0.04, with no significant *P* values conforming to a state of population expansion (Online Fig. S1). Tajima's *D*-test statistic (–2.14919, $P < 0.01$), Fu and Li's *F*-test statistic (–4.17343, $P < 0.02$), and Fu and Li's *F*-test statistic (–5.02451, $P < 0.02$) also indicated a demography consistent with the expansion model. The bimodal mismatch distribution is characteristic of populations at demographic equilibrium (Slatkin and Hudson 1991, Rogers and Harpending 1992, Excoffier 2004). In this case, however, the bimodal characteristic

Table 1. Pairwise genetic distance between specimens of spotted seatrout from 18 sampling areas from Texas to North Carolina: distance measures, Φ_{ST} [above diagonal, significant values in **bold**, after Benjamini and Hochberg false detection rate (1995)] for mtDNA control region sequences (335-bp), and D_A (below diagonal, there is no method to assess significant values for D_A) for 38 microsatellite (27 Cneb and 11 Soc) markers. Sampling area numbers 1 to 18 as in Figure 1.

Area	1	2	3	4	5	6	7	8	9	10	11	12	13	14	15	16	17	18
1	—	0.0491	0.0164	0.0276	0.0301	0.0180	0.0338	0.0246	0.0302	0.0512	0.0321	0.0282	0.0802	**0.1203**	**0.3287**	**0.2205**	**0.2496**	**0.3591**
2	0.1054	—	−0.0072	0.0053	0.0252	0.0095	0.0040	−0.0122	0.0070	0.0163	0.0145	0.0015	0.0598	0.0700	**0.2868**	**0.1650**	**0.1907**	**0.3177**
3	0.1127	0.1032	—	−0.0143	−0.0090	−0.0064	−0.0084	−0.0230	−0.0168	−0.0054	−0.0143	−0.0255	0.0554	0.0763	**0.3136**	**0.1879**	**0.2156**	**0.3430**
4	0.1174	0.1153	0.1015	—	0.0056	−0.0045	−0.0018	−0.0160	−0.0002	0.0074	0.0078	−0.0054	0.0526	0.0747	**0.2856**	**0.1683**	**0.1979**	**0.3125**
5	0.1380	0.1224	0.1157	0.1200	—	0.0146	0.0095	−0.0033	−0.0156	0.0002	−0.0111	−0.0085	0.1038	**0.1226**	**0.3731**	**0.2455**	**0.2772**	**0.4045**
6	0.1430	0.1368	0.1409	0.1358	0.1039	—	−0.0060	−0.0186	0.0023	0.0132	0.0072	−0.0045	0.0136	0.0322	**0.2308**	**0.1192**	**0.1474**	**0.2559**
7	0.1190	0.1105	0.1197	0.1003	0.0757	0.0760	—	−0.0147	−0.0027	0.0105	0.0025	−0.0053	0.0307	0.0443	**0.2264**	**0.1284**	**0.1499**	**0.2412**
8	0.1604	0.1477	0.1527	0.1451	0.1101	0.0966	0.0641	—	−0.0142	−0.0025	−0.0073	−0.0205	0.0279	0.0458	**0.2522**	**0.1381**	**0.1644**	**0.2809**
9	0.1361	0.1337	0.1417	0.1242	0.0960	0.0827	0.0528	0.0841	—	−0.0183	−0.0210	−0.0218	0.0888	0.0980	**0.3435**	**0.2181**	**0.2446**	**0.3729**
10	0.1590	0.1498	0.1530	0.1464	0.1186	0.1098	0.0795	0.1041	0.0918	—	−0.0221	−0.0171	**0.1171**	**0.1126**	**0.3779**	**0.2492**	**0.2774**	**0.4094**
11	0.1666	0.1464	0.1526	0.1470	0.1175	0.1063	0.0747	0.0936	0.0916	0.1122	—	−0.0189	**0.1044**	**0.1090**	**0.3744**	**0.2428**	**0.2755**	**0.4083**
12	0.1615	0.1614	0.1511	0.1462	0.1131	0.1089	0.0795	0.0954	0.0885	0.1051	0.1055	—	0.0689	0.0791	**0.3383**	**0.2064**	**0.2359**	**0.3701**
13	0.2169	0.2017	0.1959	0.1901	0.1603	0.1565	0.1232	0.1391	0.1448	0.1429	0.1246	0.1418	—	−0.0127	**0.1110**	**0.0198**	**0.0435**	**0.1321**
14	0.2107	0.2089	0.2046	0.2159	0.1844	0.1907	0.1801	0.1967	0.1785	0.2067	0.2026	0.1989	0.1939	—	**0.1230**	**0.0239**	**0.0500**	**0.1432**
15	0.2171	0.2099	0.2203	0.2262	0.1915	0.2125	0.1848	0.2095	0.1822	0.2025	0.2156	0.2107	0.2042	0.1024	—	0.0140	0.0079	−0.0064
16	0.2134	0.2040	0.2130	0.2197	0.1782	0.1991	0.1753	0.1995	0.1789	0.1879	0.2012	0.1996	0.1939	0.1003	0.0768	—	−0.0130	0.0281
17	0.1838	0.1808	0.1848	0.1902	0.1616	0.1839	0.1571	0.1811	0.1600	0.1821	0.1861	0.1838	0.1976	0.0848	0.0759	0.0667	—	0.0226
18	0.2393	0.2448	0.2473	0.2562	0.2148	0.2356	0.2120	0.2323	0.2158	0.2331	0.2292	0.2340	0.2366	0.1370	0.1256	0.1093	0.1148	—

is a manifestation of the two well-defined lineages, each of which, when separately analyzed, showed a perfect match with the expansion model (Online Fig. S1, the graph of only one was shown). The lineages showed a 1.61% sequence divergence, which may have originated through a bottleneck indicated by a negative Tajima's *D* (–2.45973; $P < 0.001$) and a star-like interhaplotype phylogeny tree (Fig. 2).

Microsatellite Marker Genetic Diversity Measurements.—The number of specimens analyzed for the control region and for the microsatellite markers differed slightly because some specimens from some sampling areas did not work in the control region but did in the microsatellite genotyping and vice versa. Thirteen specimens that failed to amplify in 8 microsatellite markers were removed. The average of the genetic diversity measurements over all 38 loci for each of the three regions and each sampling area are summarized in Online Table S3 and Online Table S4, respectively. The total number of unique alleles sampled from the spotted seatrout gene pool over all the microsatellite markers was 698, and, of these, an average of 335 were recorded among individuals in each sampling area for the study of genetic relatedness. For specimens from Cedar Key ($n = 117$), which were used to characterize the microsatellite markers, the average number of alleles per locus was 13.7, but 18.4 for the total 18 sampling areas ($n = 534$) (see Appendix 1). Seven loci departed from Hardy-Weinberg equilibrium in one to four sampling areas because of homozygote excess due to scoring errors resulting from stutter bands or from null alleles but no allelic dropout. Upon applying Benjamini and Hochberg's (1995) corrections, these scoring errors were 2.4% (16 out of 666) of the microsatellite locus–sampling area combinations excluding one almost monomorphic locus. This showed that the scoring quality was quite satisfactory for all analytical purposes.

Microsatellite Marker Genetic Structure.—Axis 1 of the 2-dimensional FCA strongly separated the GoM and Atlantic samples, whereas Axis 2 partly separated the eastern and western GoM specimens (Fig. 4A). No individuals from the Atlantic appear to have moved into the eastern GoM region. Similarly, the PCA scattergram based on pairwise D_A (Table 1, below diagonal) also showed that the GoM and Atlantic sampling areas were completely separated by PC1, which explained 57.5% of the variation, whereas the eastern and western sampling areas were also almost completely separated by PC2, which explained 27.3% of the genetic variation (Fig. 4B). Three groups were decidedly supported on the PCA plot, the western GoM, from Texas to Fort Walton, Florida (sampling areas 1–4); the eastern GoM (Florida GoM), from Apalachicola to Florida Bay (sampling areas 5–13) separated by coordinate 2; and the Atlantic Ocean from Sebastian Inlet to North Carolina (sampling areas 14–18).

In the overall AMOVA, 96.7% of the variation was found within sampling areas, and 3.3% among sampling areas (Table 2) indicating the existence of significant heterogeneity among sampling areas (Φ_{ST} value of 0.033, $P < 0.0001$). The highest Φ_{ST} value for any two-group division across the regions was found when the sampling areas were divided between the GoM and Atlantic regions (0.057, $P < 0.0001$). The Φ_{ST} value for the two-group division between the western and eastern GoM was also highly significant (0.013, $P < 0.002$). The greatest Φ_{ST} value among three-group divisions was found when the sampling areas were divided into the three genetic regions (clusters) as in the PCA plot (0.045, $P < 0.0001$; Table 2).

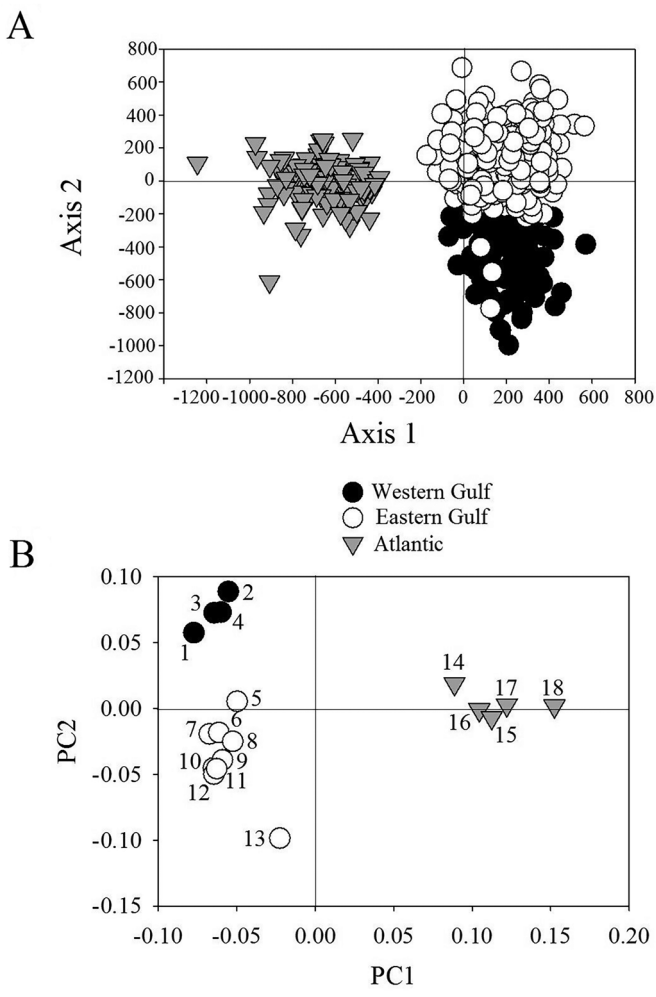

Figure 4. (A) Two-dimensional factorial correspondence analysis of 534 individuals (for spotted seatrout, *Cynoscion nebulosus*) based on 38 microsatellite loci and (B) principal coordinate analysis of 18 pairwise sampling area based on Nei's D_A. Analysis based on microsatellite markers separated the 18 sampling areas into three regions. Sampling areas number as in Figure 1.

The Mantel test conducted with the D_A distance matrix showed a significant positive relationship between genetic and geographic distances within each cluster (1: western GoM, $P = 0.027$; 2: eastern GoM, $P = 0.010$; 3: Atlantic Ocean, $P = 0.040$; Online Fig. S2). Individuals within a sampling area were genetically similar, but differences increased linearly between sampling areas as geographic distance increased.

In the STRUCTURE analysis run to detect the number of clusters among individuals, the likelihood values increased quickly from a value of $K = 1$ to a value of $K = 2$, followed by a small increase to a value of $K = 3$ before plateauing at $K = 4$ and decreasing for larger values of K [L(K); Online Fig. S3]. STRUCTURE output in STRUCTURE HARVESTER produced two peaks—the highest at $K = 2$ ($\Delta K = 1349$) and a lower peak at $K = 3$ ($\Delta K = 256$; Online Fig. S3)—indicating a hierarchical

Table 2. Analyses of molecular variance among mtDNA control region haplotypes and 38 microsatellite DNA loci genotypes of spotted seatrout (*Cynoscion nebulosus*) specimens collected from Texas to North Carolina. Sampling areas were partitioned into three groups (regions), as: western Gulf of Mexico (Samples 1–4), eastern Gulf of Mexico (samples 5–13), and Atlantic Ocean (samples 14–18).

	MtDNA control region				Microsatellite DNA loci			
Variance Component	df	Var	Φ	*P*	df	Var	Φ	*P*
All sampling areas								
Among sampling areas	17	0.27	0.098	<0.001	17	0.40	0.033	<0.001
Within sampling areas	529	2.48	–		1,050	11.76	–	
Gulf of Mexico vs Atlantic Ocean								
Between regions	1	0.58	0.186	<0.001	1	0.72	0.057	<0.001
Among sampling areas within regions	16	0.04	0.017	0.011	16	0.13	0.011	<0.001
Within sampling areas	529	2.45	0.199	<0.001	1,050	11.76	0.068	<0.001
Western Gulf of Mexico vs eastern Gulf of Mexico vs Atlantic Ocean								
Among regions	2	0.35	0.126	<0.001	2	0.56	0.045	<0.001
Among sampling areas within regions	15	0.04	0.015	0.015	15	0.05	0.004	<0.001
Within sampling areas	529	2.48	0.139	<0.001	1,050	11.76	0.049	<0.001
Western Gulf of Mexico vs eastern Gulf of Mexico								
Between regions	1	0.01	0.008	0.208	1	0.09	0.013	0.002
Among sampling areas within regions	11	0.02	0.010	0.113	11	0.04	0.006	<0.001
Within sampling areas	401	2.61	0.010	0.086	823	6.57	0.018	<0.001
Eastern Gulf of Mexico vs Atlantic Ocean								
Between regions	1	0.54	0.184	0.001	1	0.38	0.066	0.001
Among sampling areas within regions	12	0.39	0.015	0.021	12	0.06	0.005	<0.001
Within sampling areas	428	2.48	0.196	<0.001	840	6.94	0.062	<0.001

Φ-statistic: Φ_{CT}, among groups (regions); Φ_{SC}, among sampling area within regions; Φ_{ST}, within sampling areas. df = degree of freedom, Var = variance. Location of sampling area numbers is given in Figure 1.

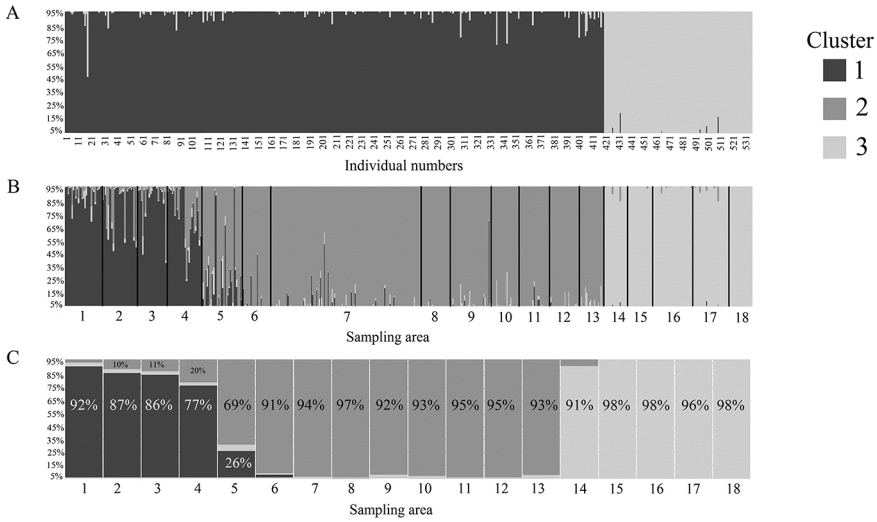

Figure 5. Population structure of the spotted seatrout (*Cynoscion nebulosus*) within the range from Texas to North Carolina specimens, according to posterior probability assignment produced by the analysis of 38 polymorphic microsatellite loci (1.0×10^6 burn-in, and 3.0×10^6 replications) with the program STRUCTURE. The output from 10 replicates from the program CLUMPP for 534 specimens from 18 sampling areas indicates (A) cluster percentage per individual for the highest modal value (number of genetic clusters) when $K = 2$ partitioning Gulf specimens 1–418 from sampling areas 1–13 and Atlantic specimens 419–534 from sampling areas 14–18; (B) cluster percentage for each individual, grouped by sampling area for the best modal value of $K = 3$ (spotted seatrout population structure); and (C) proportional values represented by each cluster within sampling areas 1–18. Cluster percentage >10% is given in each sampling area.

substructure. At $K = 2$, the spotted seatrout is partitioned between the GoM and the Atlantic sampling areas with a genetic break between Biscayne Bay (assigned to the GoM cluster) and Sebastian Inlet (assigned to the Atlantic cluster), with 97% of individual assignment to one of clusters 2 and 3 (Fig. 5A). At $K = 3$, 73%, 93%, and 100% of the individuals were assigned with >90% probability to clusters 1, 2, or 3, respectively. These clusters differentiate the spotted seatrout from Texas to North Carolina (Fig. 5B; $K = 3$), congruent with the FCA/PCA plot (Fig. 4A, B) and show that sampling area associations exist in the spotted seatrout based on geographic location in three clusters as shown in Fig. 1. The proportional values represented by each cluster within sampling areas 1–18 are shown in Fig. 5C. The averages were 0.86, 0.91, and 0.96 for clusters 1, 2, and 3, respectively. Independent STRUCTURE analysis in each of the three regions showed no finer-scale patterns.

Discussion

In coastal areas of the southeastern United States, the genetic population structure of the spotted seatrout is organized hierarchically at two levels. At the first, higher level, the GoM and Atlantic sampling areas are divided, and at the second, lower level, the GoM sampling areas are further divided, resulting in a total of three genetic stocks. In the present study, a stock is considered as a population (or geographic populations, with or without isolation by distance) that is genetically and geographically distinct by restriction of gene flow between it and adjacent such population(s) and identified as a cluster via STRUCTURE analysis. The use of STRUCTURE analysis

should not be considered a sine qua non to define a management stock. For other definitions of the stock, see Waples and Gaggiotti (2006) and Tringali et al. (2008).

The three genetic stocks of spotted seatrout defined here that satisfy our definition are: (1) a western GoM stock that extends at least from South Padre Island, Texas, to Fort Walton, Florida; (2) an eastern GoM stock that extends from Apalachicola Bay, Florida, to Biscayne Bay, Florida, just northeast of the Florida Keys; and (3) an east coast, Atlantic stock that extends from Sebastian Inlet, Florida, to the northernmost collection area at Morehead, North Carolina. Within each of those three stocks, patterns of isolation by distance were also evident, consistent with the longstanding observation of only limited dispersal of early life from their natal estuaries.

Our efforts to increase sample size at different levels (i.e., number of areas, number of individuals, and number of loci)—decidedly improved resolution of stock structure (Reiss et al. 2009, Horne et al. 2013)—but it was less evident with mtDNA than microsatellite markers. The mtDNA control region indicated a divergence between the GoM and Atlantic sampling regions at south Florida but none between the western and eastern GoM regions, whereas the microsatellite markers identified the presence of two stocks in the GoM region. While the use of microsatellites has revealed finer-scale genetic structuring in a range of marine fishes (Shaw et al. 1999, Hallerman 2003), our results have been fortified by a much larger number of loci that also incorporated species-specific microsatellite markers (see Appendix 1) than in earlier studies of the genetic population structure of the spotted seatrout (see Online Table S1).

Our effort to sample across the species' distribution may not have been sufficient at its northernmost range. A recent study using 13 microsatellite markers (O'Donnell et al. 2014) proposed a genetic break between South Carolina and North Carolina, at the region of the New River in North Carolina. This genetic break is south of the known biogeographical boundary at Cape Hatteras, which is associated with water masses of sharply differing temperatures and defines the Virginian and Carolinian provinces. We had predicted that a more likely site for a genetic break in this region would be expected to be north of Cape Hatteras, so the result of O'Donnell et al. (2014) was not expected. More specimens from the northernmost range in our study may have helped confirm this break. Likewise, the westernmost range of the spotted seatrout extends to Campeche Bay Mexico, and fish in those waters also should be examined to determine the western domain of cluster 1.

The genetic break between the GoM and Atlantic groups falls in the coastal area between Biscayne Bay and Sebastian Inlet. In the case of the spotted seatrout and other estuarine-dependent marine species [e.g., sheepshead, *Archosargus probatocephalus* (Walbaum, 1792); Seyoum et al. 2017] this genetic break occurs north of Biscayne Bay, from Miami to Palm Beach and is associated with discontinuity in estuarine habitat in this area. This estuarine gap deprives juvenile spotted seatrout of essential nursery habitat, limiting gene flow between the eastern GoM and Atlantic stocks. Spotted seatrout records are rare for this 112-km stretch (Johnson and Seaman 1986), a linear discontinuity greater than the typical range of individual spotted seatrout movements (approximately 48 km from their origin; Moffett 1961, Beaumariage 1969). This pass causes a major hurdle for the spotted seatrout to overcome and the genetic break at this region is, for this reason, more pronounced causing a deeper divergence between the GoM and Atlantic stocks than that between the western and eastern GoM stocks.

The location of the genetic break between the western and eastern GoM stocks is at Apalachicola Bay, situated within the central GoM coast vicariant zone (McClure and McEachran 1992). This is a region of genetic breaks in several benthic fishes and invertebrate species, the result of complex geographic and environmental history and variables (for discussion of hypotheses, see Bert 1986, McClure and McEachran 1992 and references therein; and Portnoy and Gold 2012). Apalachicola Bay is not an area of discontinuous estuarine habitat, but one of estuarine plasticity, in which habitats undergo cyclical changes. It is a shallow coastal lagoon fringed by barrier islands and dominated by high- and low-energy wind effect and tidal currents (Livingston 1984). Apalachicola Bay periodically floods, rapidly switching salinity from marine to almost entirely fresh water and increasing nutrient loads (Livingston et al. 2000). For example, high freshwater runoff (January–May), resulting in reduced salinity, acts as a barrier near the Apalachicola River, sharply curtailing most westward emigration of blue crabs (*Callinectes sapidus* Rathbun, 1896; Steele 1991). The Apalachicola peninsula also impedes the eastward flux of red snapper [*Lutjanus campechanus* (Poey, 1860)] larvae from the central and western GoM (Johnson et al. 2009). We postulate that temporal changes in the estuarine habitat, whether reflecting changes in salinity, wind, tidal currents, or combinations of these factors, limit gene flow between spotted seatrout groups in the eastern and western GoM. The occurrence of oceanographic barriers or potentially transient current inhibiting larval exchange between populations cannot be ruled out. These cyclical, complex changes interfere with (as opposed to impede, as in between the GoM and Atlantic break) gene flow between spotted seatrout populations on either side of the estuarine plasticity zone, causing a shallow divergence within the GoM region.

Defining stock boundaries is fundamental for continued fisheries assessment and management, which proceeds in real time, using the best available science. In the case of spotted seatrout, our literature review did not find consensus as to the number and locations of stocks. In some cases, the spatial scale of specific studies was local by design, and findings did not particularly complement those of the other studies. In other, more expansive studies, selected samples were phylogenetically misaligned with a geographically distant stock. Our experience with microsatellite markers (sheepshead; Seyoum et al. 2017) leads us to recommend species-specific markers versus nonspecific markers for investigating genetic stock of coastal species, particularly where the differentiation might be of a fine-scale nature. As we did here, a recommended field sampling design has two stages: sampling broadly at regular intervals and filling gaps later, or increasing sample sizes for areas of high genetic diversity. After adding several years of collections to our spotted seatrout database, it appears that we have reached a stable conclusion about the spotted seatrout genetic stock structure as determined by STRUCTURE.

Our approach suited our goal to address the genetic structure of spotted seatrout across a majority of this species' distribution. Further investigation of genetic structure will likely include next generation application of single nucleotide polymorphisms, which will be an appropriate, independent method to test our hypothesis for spotted seatrout. Such additional work can also be justified because of the criticism that STRUCTURE may not work very well for less differentiated populations that are below $F_{ST} = 0.02$ (Latch et al. 2006).

Our results confirm that Florida is the only state that has more than one genetic stock of spotted seatrout within its jurisdiction. Florida has already recognized two

management units—GoM and Atlantic—and assesses these units as four Florida regions (northeast, southeast, southwest, and northwest) based on preliminary genetic samples collected in coastal Florida more than a decade ago (Murphy et al. 2011). The north-south boundaries used for assessment are approximately halfway along peninsular Florida (east coast: Flagler-Volusia county line; west coast: Pinellas-Pasco county line). Strictly in terms of these new findings of genetic stock structure: (1) the east coast is unnecessarily split into two assessment units, (2) the GoM-Atlantic boundary should be moved to Biscayne Bay, and (3) the GoM assessment boundary should be moved north to Apalachicola. However, our recommendation may be tempered for other reasons, for example, if the assessment is trying to model spatial fleet differences within or across a genetic stock area. In addition, spotted seatrout management has been largely successful recently, exceeding the 35% spawning potential ratio (SPR) management goal in three regions, and close to the SPR goal in the northwest Florida region. In such favorable conditions, our recommendation is more proactive rather than of urgent concern, such as when genetic diversity is at risk when stock sizes are low. A new assessment is expected in the next year or two, at which time the ramifications of these mismatched genetic and harvest stocks can be evaluated and incorporated appropriately.

The requirement for sustainable management of spotted seatrout by regulatory agencies is likely to drive further research of this relatively data-rich species, which will be of interest to managers, ecologists, and evolutionary biologists alike. The genetic data presented herein provide geographic context of population structure, and specifically, identifying priority regions to measure mixing rates of individual spotted seatrout by tagging and testing population structure hypotheses on an ecological scale. Such familiar fisheries techniques, as part of an interdisciplinary approach (Cadrin et al. 2014, McBride 2014), should shed light on more general mechanistic processes restricting gene flow between population clusters in nearshore marine systems.

Acknowledgments

We thank the following for fish samples: the staff of the Fisheries-Independent Monitoring program, and particularly the Tequesta and Cedar Key field laboratories, of the Florida Fish and Wildlife Conservation Commission's Fish and Wildlife Research Institute, and C Crawford, C Lund, J Fortuna, D Guadagnoli, and the Low Country Anglers of South Carolina. We are especially grateful to R Grunwald, J Boyett, J Pernell for various help, and to B Barthel, T Bert, and especially B Cowder for helpful suggestions and comments of the manuscript. This work was supported by the US Department of the Interior, US Fish and Wildlife Service, under the Federal Aid in Sport Fish Restoration Program, Grant F–69. The statements, findings, and conclusions are those of the authors and do not necessarily reflect the views or policies of the Department of the Interior. Mention of trade names or commercial products does not constitute their endorsement by the US government.

Literature Cited

Anderson JD, Karel WJ. 2009. A genetic assessment of current management strategies for spotted seatrout in Texas. Mar Coast Fish. 1:121–132. https://doi.org/10.1577/C09-001.1

Anderson JD, Karel WJ. 2010. Population genetics and dynamics of spotted seatrout in the estuarine waters of Texas. Fish Aqua J. Volume 2010: FAJ–2 http://astonjournals.com/manuscripts/Vol2010/FAJ-2_Vol2010.pdf

Beaumariage DS. 1969. Returns from the 1965 Schlitz tagging program including a cumulative analysis of previous results Florida Department of Natural Resources. Marine Research Laboratory Technical Series No. 59:1–38.

Belkhir K, Borsa P, Chikhi L, Raufaste N, Bonhomme F. 2000. GENETIX 4.03, Logiciel sous Windows™ pour la génétique des populations. Laboratoire Génome, Populations, Interactions CNRS UMR 5000, Université de Montpellier II, Montpellier, France.

Benjamini Y, Hochberg Y. 1995. Controlling the false discovery rate: a practical and powerful approach to multiple testing. J R Stat Soc B. 57:289–300.

Bert TM. 1986. Speciation in western Atlantic stone crabs (genus *Menippe*): the role of geological processes and climatic events in the formation and distribution of species. Mar Biol. 93:157–170. https://doi.org/10.1007/BF00508253

Briggs JC, Bowen BW. 2012. A realignment of marine biogeographic provinces with particular reference to fish distributions. J Biogeogr. 39:12–30. https://doi.org/10.1111/j.1365-2699.2011.02613.x

Cadrin SX, Kerr LA, Mariani S. 2014. Stock Identification Methods, 2nd edn. San Diego, Academic Press. http://dx.doi.org/10.1016/B978-0-12-397003-9.00022-9

Earl DA, vonHoldt MB. 2012. STRUCTURE HARVESTER: a website and program for visualizing STRUCTURE output and implementing the Evanno method. Cons Gen Res. 4:359–361. https://doi.org/10.1007/s12686-011-9548-7

Eble JA, Bowen BW, Bernardi G. 2015. Phylogeography of coral reef fishes. *In*: Mora C, editor. Ecology of Fishes on Coral Reefs. Cambridge University Press. p. 64–75.

Escatel-Luna E, Adams DH, Uribe-Alcocer M, Islas-Villanueva V, Díaz-Jaimes P. 2015. Population genetic structure of the bonnethead shark, *Sphyrna tiburo*, from the western North Atlantic Ocean based on mtDNA sequences. J Hered. 106:355–365. https://doi.org/10.1093/jhered/esv030

Evanno G, Regnaut S, Goudet J. 2005. Detecting the number of clusters of individuals using the software STRUCTURE: a simulation study. Mol Ecol. 14:2611–2620. https://doi.org/10.1111/j.1365-294X.2005.02553.x

Excoffier L. 2004. Patterns of DNA sequence diversity and genetic structure after a range expansion: lessons from the infinite-island model. Mol Ecol. 13:853–864. https://doi.org/10.1046/j.1365-294X.2003.02004.x

Excoffier L, Lischer HEL. 2010. Arlequin suite version 3.5: a new series of programs to perform population genetics analyses under Linux and Windows. Mol Ecol Resour. 10:564–567. https://doi.org/10.1111/j.1755-0998.2010.02847.x

Excoffier L, Smouse PE, Quattro JM. 1992. Analysis of molecular variance inferred from metric distances among DNA haplotypes: application to human mitochondrial DNA restriction data. Genetics. 131:479–491.

Gold JR, Richardson LR. 1998. Mitochondrial DNA diversification and population structure in fishes from the Gulf of Mexico and western Atlantic. J Hered. 89:404–414. https://doi.org/10.1093/jhered/89.5.404

Gold JR, Richardson LR, Furman C. 1999. Mitochondrial DNA diversity and population structure of spotted seatrout (*Cynoscion nebulosus*) in coastal waters of the southeastern United States. Gulf Mex Sci. 1999:40–50.

Gold JR, Stewart LB, Ward R. 2003. Population structure of spotted seatrout (*Cynoscion nebulosus*) along the Texas Gulf Coast, as revealed by genetic analysis. *In*: Bortone SA, editor. Biology of the Spotted Seatrout. Boca Raton, Florida, CRC Press. p. 17–29.

Goudet J. 2001. FSTAT, a program to estimate and test gene diversities and fixation indices version 2.9. http://www2.unil.ch/popgen/softwares/FSTat.htm

Hallerman EM. 2003. Population genetics: principles and applications for fisheries scientists. Bethesda, Maryland, American Fisheries Society. 475 p.

Harpending RC. 1994. Signature of ancient population growth in a low-resolution mitochondrial DNA mismatch distribution. Hum Biol. 66:591–600.

Horne JB, Momigliano P, van Herwerden L, Newman SJ. 2013. Murky waters: searching for structure in genetically depauperate blue threadfin populations of Western Australia. Fish Res. 146:1–6. https://doi.org/10.1016/j.fishres.2013.03.013

Iversen ES, Moffett AW. 1962. Estimation of abundance and mortality of a spotted seatrout population. Trans Am Fish Soc. 91:395–398. https://doi.org/10.1577/1548-8659(1962)91[395:EOAAMO]2.0.CO;2

Jakobsson M, Rosenberg N. 2007. CLUMPP: a cluster matching and permutation program for dealing with label switching and multimodality in analysis of population structure. Bioinformatics. 23:1801–1806. https://doi.org/10.1093/bioinformatics/btm233

Johnson DR, Seaman W. 1986. Species profiles: life histories and environmental requirements of coastal fish and invertebrates (South Florida) – spotted seatrout. US Fish and Wildlife Series Biological Report. 82(11.72). US Army Corps of Engineers TR EL–82–4. Lafayette, Louisiana.

Johnson DR, Perry HM, Lyczkowski–Shultz J, Hanisko D. 2009. Red snapper larval transport in the northern Gulf of Mexico. Trans Am Fish Soc. 138:458–470. https://doi.org/10.1577/T08-008.1

Kalinowski ST, Taper ML, Marshall TC. 2007. Revising how the computer program CERVUS accommodates genotyping error increases success in paternity assignment. Mol Ecol. 16:1099–1106. https://doi.org/10.1111/j.1365-294X.2007.03089.x

King TL, Pate HO. 1992. Population structure of spotted seatrout inhabiting the Texas Gulf Coast: an allozymic perspective. Trans Am Fish Soc. 121:746–756. https://doi.org/10.1577/1548-8659(1992)121<0746:PSOSSI>2.3.CO;2

King TL, Zimmerman EG. 1993. Clinal variation at aspartate aminotransferase-2 in spotted seatrout, *Cynoscion nebulosus* (Cuvier), inhabiting the north-western Gulf of Mexico. Anim Genet. 24:59–61. https://doi.org/10.1111/j.1365-2052.1993.tb00920.x

Kocher TD, Thomas WK, Meyer A, Edwards SV, Pääbo S, Villablanca FX, Wilson AC. 1989. Dynamics of mitochondrial DNA evolution in animals: amplification and sequencing with conserved primers. Proc Natl Acad Sci USA. 86:6196–6200. https://doi.org/10.1073/pnas.86.16.6196

Latch EK, Dharmarajan G, Glaubitz JC, Rhodes OE Jr. 2006. Relative performance of Bayesian clustering software for inferring population substructure and individual assignment at low levels of population differentiation. Cons Gene. 7:295–302. https://doi.org/10.1007/s10592-005-9098-1

Librado P, Rozas J. 2009. DNaSP version 5: a software for comprehensive analysis of DNA polymorphism data. Bioinformatics. 25:1451–1452. https://doi.org/10.1093/bioinformatics/btp187

Livingston RJ. 1984. The ecology of the Apalachicola Bay system: an estuarine profile. US Fish and Wildlife Service. FWS/OBS 82/05. 148 p.

Livingston RJ, Lewis FG, Woodsum GC, Niu XF, Galperin B, Huang W, Christensen JD, Monaco ME, Battista TA, Klein CJ, et al. 2000. Modeling oyster population response to variation in freshwater input. Estuar Coast Shelf Sci. 50:655–672. https://doi.org/10.1006/ecss.1999.0597

Mach M, Sbrocco E, Hice L, Duffy T, Conover D, Barber P. 2011. Regional differentiation and post-glacial expansion of the Atlantic silverside, *Menidia*, an annual fish with high dispersal potential. Mar Biol. 158:515–530. https://doi.org/10.1007/s00227-010-1577-3

McBride R. 2014. Managing a marine stock portfolio: stock identification, structure, and management of 25 fishery species along the Atlantic coast of the United States. N Am J Fish Manage. 34:710–734. https://doi.org/10.1080/02755947.2014.902408

McCartney MA, Burton ML, Lima TG. 2013. Mitochondrial DNA differentiation between populations of black sea bass (*Centropristis striata*) across Cape Hatteras, North Carolina (USA). J Biogeogr. 40:1386–1398. https://doi.org/10.1111/jbi.12103

McClure MR, McEachran JD. 1992. Hybridization between *Prionotus alatus* and *P. paralatus* in the northern Gulf of Mexico (Pisces: Triglidae). Copeia. 1992:1039–1046. https://doi.org/10.2307/1446635

Meyer A, Kocher TD, Basasibwaki P, Wilson AC. 1990. Monophyletic origin of Victoria cichlid fishes suggested by mitochondrial DNA sequences. Nature. 347:550–553. https://doi.org/10.1038/347550a0

Moffett AW. 1961. Movements and growth of spotted seatrout, *Cynoscion nebulosus* (Cuvier), in west Florida. Florida State Board of Conservation Technical Series. 36:1–35.

Murphy MD, Chagaris D, Addis D. 2011. An assessment of the status of spotted seatrout in Florida waters through 2009. Florida Fish and Wildlife Conservation Commission, Fish and Wildlife Research Institute, Report IHR 2011-002. St. Petersburg, Florida.

NMFS (National Marine Fisheries Service). 2014. Fisheries of the United States, 2013. NMFS, Silver Spring, Maryland, Office of Science and Technology, Fisheries Statistics Division. http://www.st.nmfs.noaa.gov/Assets/commercial/fus/fus13/02_commercial 2013.pdf

Nei M, Tajima F, Tateno Y. 1983. Accuracy of estimated phylogenetic trees from molecular data. J Mol Evol. 19:153–170. https://doi.org/10.1007/BF02300753

O'Donnell TP, Denson MR, Darden TL. 2014. Genetic population structure of spotted seatrout *Cynoscion nebulosus* along the south-eastern U.S.A. J Fish Biol. 85:374–393. https://doi.org/10.1111/jfb.12419

Peakall R, Smouse PE. 2006. GENALEX 6: genetic analysis in Excel. Population genetic software for teaching and research. Mol Ecol Notes. 6:288–295. https://doi.org/10.1111/j.1471-8286.2005.01155.x

Peakall R, Smouse PE. 2012. GenAlEx 6.5: genetic analysis in Excel. Population genetic software for teaching and research – an update. Bioinformatics. 28:2537–2539. https://doi.org/10.1093/bioinformatics/bts460

Pearson JC. 1929. Natural history and conservation of the redfish and other commercial sciaenids on the Texas coast. Fish Bull. 44:129–214.

Peebles EB, Tolley SG. 1988. Distribution, growth and mortality of larval spotted seatrout, *Cynoscion nebulosus*: a comparison between two adjacent estuarine areas of southwest Florida. Bull Mar Sci. 42:397–410.

Portnoy DS, Gold JR. 2012. Evidence of multiple vicariance in a marine suture-zone in the Gulf of Mexico. J Biogeogr. 39:1499–1507. https://doi.org/10.1111/j.1365-2699.2012.02699.x

Pritchard JK, Stephens M, Donnelly P. 2000. Inference of population structure using multilocus genotype data. Genetics. 155:945–959.

Pritchard JK, Wen X, Falush D. 2009. Documentation for Structure software: Version 2.2. Chicago, University of Chicago Press. http://pritch.bsd.uchicago.edu/software

Ramsey PR, Wakeman JM. 1987. Population structure of *Sciaenops ocellatus* and *Cynoscion nebulosus* Pisces: Sciaenidae): biochemical variation, genetic subdivision and dispersal. Copeia. 1987:682–695. https://doi.org/10.2307/1445660

Reiss H, Hoarau G, Dickey-Collas M, Wolff WJ. 2009. Genetic population structure of marine fish: mismatch between biological and fisheries management units. Fish Fish. 10:361–395. https://doi.org/10.1111/j.1467-2979.2008.00324.x

Renshaw AM, Gawriluk TR, Gold JR. 2009. Characterization of red drum microsatellite markers in spotted seatrout. N Amer J Aquaculture. 71:374–379. https://doi.org/10.1577/A08-070.1

Rogers AR, Harpending HC. 1992. Population growth makes waves in the distribution of pairwise genetic differences. Mol Biol Evol. 9:552–569.

Rousset F. 2008. Genepop'007: a complete reimplementation of the GenePop software for Windows and Linux. Mol Ecol Resour. 8:103–106. https://doi.org/10.1111/j.1471-8286.2007.01931.x

Seyoum S, Barthel LB, Tringali MD, Carney SL. 2013. Phylogenetic relationships among four western Atlantic *Cynoscion* species based on DNA sequences from 11 nuclear introns,

two mitochondrial genes, and genotypes from 32 microsatellite markers. Gulf Mex Sci. 31:40–49.

Seyoum S, Collins AB, Puchutulegui C, McBride RS, Tringali MD. 2015. Genetically determined population structure of hogfish (Labridae: *Lachnolaimus maximus*) in the southeastern United States. Fish Bull. 113:442–455. https://doi.org/10.7755/FB.113.4.7

Seyoum S, McBride RS, Puchutulegui C, Dutka-Gianelli J, Alvarez AC, Panzner K. 2017. Genetic population structure of a coastal marine fish (Sheepshead; *Archosargus probatocephalus* [Sparidae]) in the southeastern United States: multiple population clusters based on species-specific microsatellite markers. Bull Mar Sci. 93:691–713. https://doi.org/10.5343/bms.2016.1069

Seyoum S, Tringali MD, Bert TM, McElroy D, Stokes R. 2000. An analysis of genetic population structure in red drum (*Sciaenops ocellatus*) based on mtDNA control region sequences. Fish Bull. 127:138.

Shaw PW, Turan C, Wright JM, O'Connell M, Carvalho GR. 1999. Microsatellite DNA analysis of population structure in Atlantic herring (*Clupea harengus*), with direct comparison to allozyme and mtDNA RFLP analyses. Heredity. 83:490–499. https://doi.org/10.1038/sj.hdy.6885860

Slatkin M, Hudson RR. 1991. Pairwise comparisons of mitochondrial DNA sequences in stable and exponentially growing populations. Genetics. 129:555–562.

Somerset CR, Saillant EA. 2014. Regional population structure and management of aquaculture for stock enhancement of the spotted seatrout (*Cynoscion nebulosus*). Aquaculture. 433:66–73. https://doi.org/10.1016/j.aquaculture.2014.05.033

Steele P. 1991. Population dynamics and migration of the blue crab, *Callinectes sapidus* (Rathbun), in the eastern Gulf of Mexico. Proc Gulf Caribb Fish Inst. 40:241–244.

Takezaki N, Nei M. 1996. Genetic distances and reconstruction of phylogenetic trees from microsatellite DNA. Genetics. 144:389–399.

Takezaki N, Nei M. 2008. Empirical tests of the reliability of phylogenetic trees constructed with microsatellite DNA. Genetics. 178:385–392. https://doi.org/10.1534/genetics.107.081505

Takezaki N, Nei M, Tamura K. 2010. POPTREE2: software for constructing population trees from allele frequency data and computing other population statistics with Windows interface. Mol Biol Evol. 27:747–752. https://doi.org/10.1093/molbev/msp312

Tamura K, Stecher G, Peterson D, Filipski A, Kumar S. 2013. MEGA7: molecular evolutionary genetics analysis version 7.0. Mol Biol Evol. 30:2725–2729. https://doi.org/10.1093/molbev/mst197

Tringali MD, Seyoum S, Wallace EM, Higham M, Taylor RG, Trotter AA, Whittington JA. 2008. Limits to the use of contemporary genetic analyses in delineating biological populations for restocking and stock enhancement. Rev Fish Sci. 16:111–116. https://doi.org/10.1080/10641260701686887

Turner TF, Richardson LR, Gold JR. 1998. Polymorphic microsatellite DNA markers in red drum (*Sciaenops ocellatus*). Mol Ecol Notes. 7:1771–1773. https://doi.org/10.1046/j.1365-294x.1998.00501.x

Van Oosterhout C, Hutchinson WF, Wills DPM, Shipley P. 2004. MICROCHECKER: software for identifying and correcting genotyping errors in microsatellite data. Mol Ecol Notes. 4:535–538. https://doi.org/10.1111/j.1471-8286.2004.00684.x

Waples RS, Gaggiotti O. 2006. What is a population? An empirical evaluation of some genetic methods for identifying the number of gene pools and their degree of connectivity. Mol Ecol. 15:1419–1439. https://doi.org/10.1111/j.1365-294X.2006.02890.x

Ward R, Bowers K, Hensley R, Mobley B, Belouski E. 2007. Genetic variability in spotted seatrout (*Cynoscion nebulosus*), determined with microsatellite markers. Fish Bull. 105:197–206.

Wiley BA, Chapman RW. 2003. Population structure of spotted seatrout, *Cynoscion nebulosus*, along the Atlantic Coast of the U.S. *In:* Bortone SA, editor. Biology of the spotted seatrout. Boca Raton, Florida, CRC Press. p. 31–40.

Williams DA, Brown SD, Crawford DL. 2008. Contemporary and historical influences on the genetic structure of the estuarine-dependent Gulf killifish *Fundulus grandis.* Mar Ecol Prog Ser. 373:111–121. https://doi.org/10.3354/meps07742

Weinstein MP, Yerger RW. 1976. Electrophoretic investigation of subpopulations of the spotted seatrout, *Cynoscion nebulosus* (Cuvier), in the Gulf of Mexico and Atlantic coast of Florida. Comp Biochem Physiol B. 54:97–102. https://doi.org/10.1016/0305-0491(76)90063-8

Weir BS, Cockerham CC. 1984. Estimating *F*-statistics for the analysis of population structure. Evolution. 38:1358–1370.

Appendix 1. Characterization of 38 polymorphic microsatellite loci (27 Cneb and 11 Soc) in 117 specimens of the spotted seatrout (*Cynoscion nebulosus*) from Cedar Key, Florida. The markers for the spotted seatrout (Cneb) were developed in-house at FWC (Fish and Wildlife Research Institute by S. Seyoum) and the 11 red drum (Soc) markers were adopted [(Soc099, 133, and 243; Turner et al. 1998): (Soc415, 416, 532, 564, 568, 635, and 660; Renshaw et al. 2009)]. The allele size range and number of alleles are also given for the total number of spotted seatrout specimens collected from Texas to North Carolina from 18 sampling areas.

			Cedar Key, Florida $n = 117$					Total data $n = 534$		
Locus	Primer sequence (5′→ 3′) Forward/Reverse	Repeat motif	Allele size range	K_a	PIC	H_O	H_E	Allele size range	K_a	GenBank Accession No
Cneb01	GATTCAATTGTCTCCAAGTTAGAGGT AATGCAATGAATGCAGGGAAC	$(CG)_3(CA)_{10}$	165–179	8	0.78	0.76	0.81	161–187	13	JF495373
Cneb03	AGGAGTGTTCCCAAACACAGTTAGT TTCTGTTGCCATTCTATTCAGCTCT	$(AC)_{39}$	151–227	32	0.95	0.94	0.96	151–255	44	JF495374
Cneb04	GGAATGTTAAAAGTGAAACATGACAG CAGTGTTTCTTGCCTTTTGTACTATC	$(TG)_{18}(GA)_5$	161–185	12	0.80	0.80	0.83	139–189	16	JF495375
Cneb06	TAAAGACAGGAGTGAAAGGCTCATT ACTGTCACACTCTGGACACACAATC	$(GT)_{13}$	178–192	7	0.59	0.63	0.65	176–204	10	JF495377
Cneb07	CTCTGAAACATCGCTCCATTACTC GTCAATCAACAAGCCAACATCACT	$(GT)_{12}$	116–130	8	0.75	0.68	0.78	106–134	10	JF495378
Cneb09	TCATTCGTGTCTTAATGTAATCAGTG ACTCAGTGCCCTCTACAACTACCTC	$(CA)_{15}$	177–197	9	0.77	0.71	0.80	175–219	15	JF495379
Cneb12	CAAGTTGTTTTCTCCCTTCCATC CTCCAATGAGGCTGCACTTTTT	$(TC)_{10}$	141–173	11	0.74	0.74	0.77	141–177	15	JF495380
Cneb15	AAGCTGATGTGATGAGTGAATTTG ATTAGTGGGGTTAGAGCCTCTCATT	$(AC)_{10}$	101–105	3	0.49	0.50	0.57	93–111	8	JF495382
Cneb20	CAAACAGACTACAAATAAAGCTGGAG ATTGTTTCATGTTGGACCTGCTTAG	$(CA)_8$	185–191	4	0.36	0.43	0.44	179–193	7	JF495384
Cneb21	AGCGTCACTTAAACACAACAAGTAAC GTCCTCCTCCTCCTCCTTTCAC	$(AG)_{11}$	146–160	6	0.23	0.17	0.24	140–168	8	JF495385
Cneb22	TGAGTAAATAAGAGCAAGGGGAAATA AGTACAGTGGCAAAGAAACACACAC	$(TG)_{10}$	105–127	11	0.73	0.77	0.76	101–135	17	JF495386
Cneb23	CGAGCTAACAAGTCTTTGTGAGGAG GCTCATACTGTCAACTCTCTCACTGT	$(GA)_{14}$	127–147	9	0.67	0.60	0.71	117–149	15	JF495387
Cneb24	CTCATTGGACAAGACAGGACAC CTGGGTTTCTCTCTTTCCCTCTC	$(GA)_{10}$	110–154	23	0.85	0.88	0.87	110–158	24	JF495388
Cneb25	AATTAGCGGACATGACAGTCTCAG CTTACAGCGAGGGCTACGTTTATTA	$(TG)_{10}(GT)_5$	133–177	20	0.82	0.83	0.84	131–177	23	JF495389

Appendix 1. *Continued*.

Locus	Primer sequence (5′→ 3′) Forward/Reverse	Repeat motif	Cedar Key, Florida $n = 117$ Allele size range	K_a	PIC	H_O	H_E	Total data $n = 534$ Allele size range	K_a	GenBank Accession No
Cneb26	GTTTTGTACAGACAACTGGAGACATT AGCGTGTCTGCATATAATACATCTG	$(TG)_{24}$	106–182	32	0.94	0.97	0.95	104–184	38	JF495390
Cneb29	ATCAGCCCTGTCACTCAATGTT GAGAAAAGATCTTCTATAGGAATGAGG	$(CA)_{12}$	102–110	4	0.09	0.09	0.09	102–110	5	JF495392
Cneb30	CGAGAGAAAGAGAGACAAAGAAAAAC GGATCTCACTGGCCTCTATTACTG	$(CA)_7$	158–166	3	0.25	0.28	0.29	156–170	8	JF495393
Cneb31	CCGAGCTGCACATAAAACAAAG CATTGTGTGTGTGTGTTTTTGAA	$(CA)_8$	85–103	10	0.77	0.74	0.80	85–105	11	JF495394
Cneb32	ACAACCACAACCACCACCATC CAGGCACAGAGGAGACAGACAT	$(CT)_{11}$	107–119	6	0.20	0.21	0.21	107–123	8	JF495395
Cneb33	ACAAAAACACATGCCTATACACAAAC RAATCACCCTTGTGTTTTCATACATA	$(AC)_{16}$	123–155	17	0.84	0.54	0.86*	111–161	25	JF495396
Cneb35	GACCATCCTTGACCTCCTCTTCTA GGGTGTGTAGACAAGGAATAGG	$(CA)_{13}$	100–128	16	0.87	0.90	0.88	88–128	21	JF495398
Cneb36	ACGGATGGCCTCTCAAGGT GGCCGTCTTGTGTGTCAGG	$(GT)_{12}$	116–178	23	0.92	0.92	0.93	110–178	31	JF495399
Cneb37	TACTGTTAATTATTACGTGAGCCTGA ATGCACTTTTTCAACAGTTTCTCTC	$GA)_5/(GA)_4$ $/(GA)_7/(GA)_7$	139–193	13	0.55	0.55	0.58	139–193	18	JF495400
Cneb38	CTGACTAAAGATGGAGGAGGACAAT AGTTTGTAATATGAGTTCAGGTGCAG	$(CA)_{11}$	169–187	8	0.56	0.64	0.64	159–191	14	JF495401
Cneb39	GAGTCCCAGAGCCCATCAGA CACAGCTGAGGAGTTTGTTTCAT	$(CA)_{12}$	129–153	10	0.72	0.78	0.76	123–153	14	JF495402
Cneb40	TACAAACCTCATCACAATTCTGACAT TCTGAATTAAAATTTTCAGTTGGATTT	$(CA)_{21}$	149–177	16	0.88	0.65	0.89*	149–181	17	JF495403
Cneb41	ACTTGATTAACTCCACTGTAGCAGAA CCACCCCCACTCATTGAT	$TC)_2(CT)3_C$ $(CT)_7$	156–170	7	0.32	0.31	0.34	147–180	13	JF495404
Soc99	CACCCACTGACACACACATACAC GGAACCAATATGTCTGCCATGAT	$(CA)_{23}$	147–173	11	0.78	0.71	0.81	147–175	15	AF73272
Soc133	CATTTGGACCATCGCTACTGCTG CTTGGCATTTCCAGACATCACTG	$(TGC)_8$	190–202	6	0.41	0.39	0.43	194–208	9	AF73276
Soc243	GACGGGGATGCCATCTGC AATGCGAAAAAGACGAAACAGT	$(CCT)_9$	101–111	5	0.43	0.43	0.50	91–113	8	AF73283

Appendix 1. *Continued.*

Locus	Primer sequence (5′→ 3′) Forward/Reverse	Repeat motif	Cedar Key, Florida $n = 117$ Allele size range	K_a	PIC	H_O	H_E	Total data $n = 534$ Allele size range	K_a	GenBank Accession No
Soc415	CTCAGCACCCTCAGACATATGG CACAAGTTAAGTGGTATCGAGT	$(TG)_{15}$	184–256	27	0.89	0.91	0.91	184–260	36	AY161020
Soc416	CTCGATACCACTTAACTTGT ATCGACATAATCTGGCACCA	$(GA)_{38}$	140–194	19	0.89	0.92	0.90	140–194	27	AY161020
Soc426	GAGAGGACGTGAGCTGCTGA TGAGAAACAGAAACAGAAGGT	$(CA)_{11}$	116–190	17	0.85	0.79	0.86	116–190	23	AY161028
Soc532	GAGTGCTCACAAAGTGCCAG GTGCCAGATAGATGCTGACG	$(CA)_{14}$	108–138	16	0.85	0.81	0.87	108–138	17	EF609037
Soc564	TGCCAGCATCCGTCTACTCA AAGAGCCGACCAATCAGAGAG	$(CA)_{15}$	152–196	20	0.83	0.79	0.85	140–206	26	EF609063
Soc588	TGAATGACTTGCTTTGCTGAA AATAACCCCCACCTCTCCCT	$(GA)_{22}$	155-205	21	0.91	0.86	0.92	153–207	27	EF609084
Soc635	CATCAGCACGGTTATTTTCTTG CCTCTCTCTTTTCTTCCCTCG	$(CA)_{23}$	216–248	17	0.88	0.86	0.89	216–258	21	EU015887
Soc660	TTGCCAATGTTCTTTCTCTCT ATTCCTACTCCTGCCAAGAT	$(CA)_{12}CT(CA)_2$ AA$(CA)_5$	72–160	35	0.89	0.85	0.90	72–162	41	EU015911
Mean				13.7	0.69	0.67	0.70		18.4	

K_a = number of alleles; H_O = observed heterozygosity; H_E = expected heterozygosity; * indicates significant departure from HWE; PIC = polymorphic information content. Because of the presence of population structure in the total data, departures from Hardy-Weinberg proportions and other genetic indices are not given.